



Missouri University of Science and Technology  
**Scholars' Mine**

---

Electrical and Computer Engineering Faculty  
Research & Creative Works

Electrical and Computer Engineering

---

01 Jul 2007

## Steady State Formulation of FACTS Devices Based on AC/AC Converters

J. M. Ramirez

J. M. Gonzalez

Mariesa Crow

*Missouri University of Science and Technology, [crow@mst.edu](mailto:crow@mst.edu)*

Follow this and additional works at: [https://scholarsmine.mst.edu/electrical\\_and\\_computer\\_engineering\\_facwork](https://scholarsmine.mst.edu/electrical_and_computer_engineering_facwork)

 Part of the [Electrical and Computer Engineering Commons](#)

---

### Recommended Citation

J. M. Ramirez et al., "Steady State Formulation of FACTS Devices Based on AC/AC Converters," *IET Generation, Transmission & Distribution*, vol. 1, no. 4, pp. 619-631, Institute of Electrical and Electronics Engineers (IEEE), Jul 2007.

The definitive version is available at <https://doi.org/10.1049/iet-gtd:20060329>

This Article - Conference proceedings is brought to you for free and open access by Scholars' Mine. It has been accepted for inclusion in Electrical and Computer Engineering Faculty Research & Creative Works by an authorized administrator of Scholars' Mine. This work is protected by U. S. Copyright Law. Unauthorized use including reproduction for redistribution requires the permission of the copyright holder. For more information, please contact [scholarsmine@mst.edu](mailto:scholarsmine@mst.edu).

# Steady state formulation of FACTS devices based on ac/ac converters

J.M. Ramirez, J.M. González and M.L. Crow

**Abstract:** Here the analysis on the inclusion of a pulse width modulated (PWM) ac link unified power flow controller into a power flow program is discussed. Similarly, a PWM series compensator is connected to the power system to regulate the active power flow on the corresponding transmission line. Details of the Newton–Raphson’s power flow algorithm are exhibited. Results of simulation are presented on a 39-buses power system.

## 1 Introduction

Power systems are experiencing significant changes in the areas of control and operation, as a result of deregulation and re-structuring. The open access power market requires the power transmission and distribution to be more reliable, flexible and economical [1]. In the traditional power transmission system, controllable devices are restricted to the slow mechanism such as transformer tap changers and switched capacitors. In the late 1980s, thanks to the major developments in the semiconductor technology, it became possible to apply power electronics in the control of power systems. This led to a new field of research, known as flexible ac transmission systems (FACTS).

The FACTS incorporates power electronics-based controllers to enhance the controllability and increase the power transfer capability [2–5]. The implementation of FACTS devices requires technology for high power electronics with real-time operating control. The objectives of FACTS devices are 3-fold:

- To increase the power transfer capability of transmission systems.
- To keep power flow over designated routes.
- To realize overall system optimisation control.

FACTS devices have shown very promising results when used to improve power system steady state performance. Through the modulation of bus voltage, phase shift between buses, and transmission line reactance, static VAR compensators, thyristor-controlled phase shifters, and thyristor-controlled series capacitors, respectively, can cause a substantial increase in power transfer limits during steady-state while improving the transient behaviour [6–16].

In many applications, to hold electric power with frequency, magnitude and phase different from the one given by the source is required. The ac/ac converters’ take

charge of conditioning the energy provided by the source to the necessities of magnitude, frequency and phase that the load demands. In a first classification it is possible to distinguish two major types of ac/ac converters: (1) Direct ac/ac converters: they carry out the conversion in a single stage. (2) Indirect ac/ac converters: they carry out the conversion in two stages, through an element of energy storage (dc-link). In such converters, as the conversion is accomplished by means of the cascade connection of a rectifier, controlled or not and of an inverter, the performance it will be limited, fundamentally to high commutating frequencies.

Within the direct ac/ac converters three types of devices can be distinguished: (1) Voltage regulators (ac voltage controllers): they only allow the modification of the output magnitude, neither of the output frequency nor of the input power factor. These converters operate in natural commutation. (2) Cycloconverters in natural commutation: they are built using thyristors in natural commutation. They allow the modification of the magnitude and of the output frequency, but they do not allow to control the input power factor. These devices are also called line commutated converters. (3) Direct ac/ac converters (matrix converter): they use static devices in forced commutation, typically IGBTs. These converters allow the modification of the magnitude and of the output frequency; they are able to control the input power factor.

A direct ac/ac converter operates in forced commutation; it uses a series of bidirectional power devices as main elements of conversion. Thus, its control allows to create a controllable output voltage without restriction of frequency (UFC, unrestricted frequency changers). Such converters accomplished the ac/ac conversion without necessity of a dc link and they do not require huge elements of energy storage. An important point in the direct ac/ac converters is to have controllable power switches with operating capacity in the four quadrants. The original UFCs based-devices used thyristors with external circuits of forced commutation to implement such switches. With this solution, the power circuit was complex, voluminous, inefficient. In spite of the earlier mentioned, it was established that if the converter had bidirectional power switches, its operating principle could extend until covering a wide range of frequency.

Conventional FACTS devices are based on dc/ac converters. However, in recent years new devices based on ac/ac converters have been proposed [17–19]. These do not

© The Institution of Engineering and Technology 2007

doi:10.1049/iet-gtd:20060329

Paper first received 14th August and in revised form 20th November 2006

J.M. Ramirez and J.M. González are with CINVESTAV – Guadalajara. Av., Científica 1145. Col. El Bajío, Zapopan, Jal., 45010, Mexico

M.L. Crow is Associate Professor of Electrical Engineering, 233 Emerson Electric Co. Hall, University of Missouri-Rolla, Rolla, MO 65409-0040

E-mail: jramirez@gdl.cinvestav.mx

require a dc link, and it is possible to reach similar objectives to those obtained by means of conventional FACTS devices.

The ac/ac power converter connects supply ac utility to output ac load through only controlled bi-directional switches. The output ac signals with adjustable magnitude and frequency are constructed by single-stage power conversion process. The direct ac/ac power conversion leads to a distinct structure with no large dc-link energy storage components. Consequently, the topology can be implemented with compact size and volume compared with the diode rectifier based PWM-VSC, where the dc-link capacitor generally occupies 30–50% of the entire converter size and volume. This feature is very promising to the modern low-volume converter trend with high silicon integration. In addition to its compact design, it can draw sinusoidal input currents with unity displacement factor as well as sinusoidal output currents. The converter provides inherent bi-directional power flow capability so that load energy can be regenerated back to the supply [20, 21].

### 1.1 $\Gamma$ -Controller

Vector switching converters (VeSC) have been proposed as a versatile type of FACTS device capable of regulating power flow at an interconnection point with an arbitrary number of branches in a complex system [17].

The schematic diagram of the vector-switching converter applied as a PWM ac link unified power flow controller (UPFC) is illustrated in Fig. 1 ( $\Gamma$ -controller) [18]. The  $\Gamma$ -controller can be considered to be the ac link counterpart of the conventional UPFC system based on dc link voltage source converters (VSC). It is based on the technology of phase-shifting transformers with solid-state electronic control using PWM.

For such devices a reachable capacity is visualised to accomplish complex power flow control, redistribution of trajectories, and voltage support, whose limit values will be determined by the capacity of the required transformers, as well as of the selected power electronic devices with bidirectional capacity. Their use will be justified on the basis of the importance of the connection where they are installed, either with electrical energy commercialisation or with control purposes. Also, their employment with additional objectives, for instance, the enhancement of the damping of power oscillations is foreseeable.

The system is configured by including a shunt phase-shifting transformer (SPT), filter capacitors (FC), a quadruple-throw single-pole three-phase VeSC and a

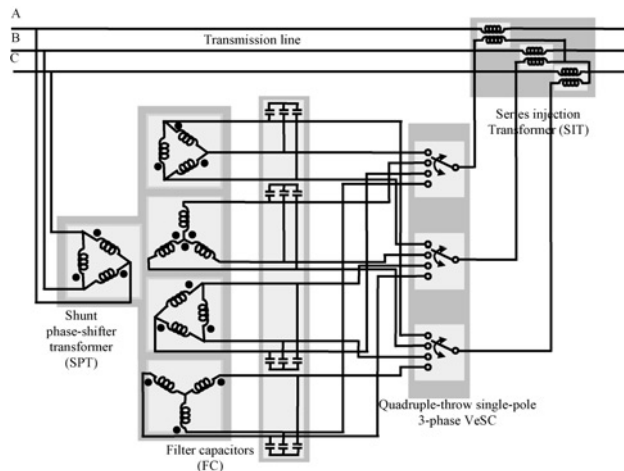


Fig. 1  $\Gamma$ -controller scheme

series injection transformer (SIT). This system may be located at any point throughout the line.

Let us assume that transformers SPT and SIT are ideal and have a unity transformation ratio. Furthermore, let us assume that the reactive power injection at the fundamental frequency due to bank CF is negligible.

The switching function  $H_i(t)$  of a throw connecting voltage  $V$  to the current  $I$  is defined as

$$H_i(t) = \begin{cases} 1 & \text{if switch } t_i \text{ is closed} \\ 0 & \text{otherwise} \end{cases} \quad (1)$$

The dc component of the switching functions may be represented by the duty ratio of the particular throw, where the duty ratio of the  $i$ th throw is defined by

$$d_i(\tau) = \frac{1}{T} \int_{\tau-T}^{\tau} H_i(t) dt \quad \text{for } i = 1, 2, \dots, N \quad (2)$$

being  $T$  the switching period. Fig. 2 can be used to conclude that

$$\sum_{i=1}^N d_i(t) = 1 \quad (3)$$

The transformation ratio of the  $\Gamma$ -connected transformer becomes a complex quantity reflecting the simultaneous phase-shifting introduced by the SPT [18]. Fig. 3 represents a single-phase scheme of the SPT in Fig. 1. The voltage  $V_{\text{out}}$  is

$$V_{\text{out}} = v_1 + v_2 + v_3 + v_4 \quad (4)$$

Besides

$$\begin{aligned} \frac{V_{\text{in}}}{v_1} &= \frac{1}{d_1}; & \frac{V_{\text{in}}}{v_2} &= \frac{1}{jd_2}; \\ \frac{V_{\text{in}}}{v_3} &= \frac{1}{-d_3}; & \frac{V_{\text{in}}}{v_4} &= \frac{1}{-jd_4} \end{aligned} \quad (5)$$

Thus

$$\begin{aligned} v_1 &= d_1 V_{\text{in}}; & v_2 &= jd_2 V_{\text{in}}; \\ v_3 &= -d_3 V_{\text{in}}; & v_4 &= -jd_4 V_{\text{in}} \end{aligned} \quad (6)$$

and

$$V_{\text{out}} = (d_1 + jd_2 - d_3 - jd_4) V_{\text{in}} = D V_{\text{in}} \quad (7)$$

where

$$D = d_1 - d_3 + j(d_2 - d_4) = d_{13} + jd_{24} \quad (8)$$

where  $d_i$  is the duty ratio of the  $i$ th throw; additionally as (3) indicates

$$d_1 + d_2 + d_3 + d_4 = 1 \quad (9)$$

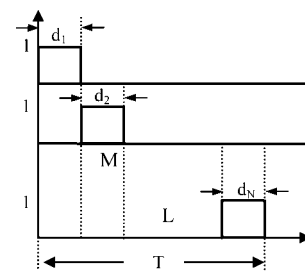
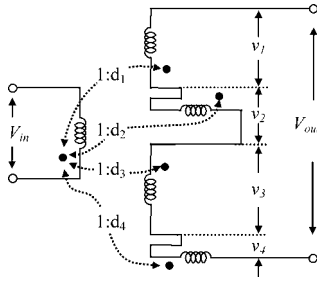


Fig. 2 Duty cycle of  $N$  switchings



**Fig. 3** SPTs single-phase equivalent

By choosing appropriate values for  $d_{13}$  and  $d_{24}$ , it is possible to control either  $(P, Q_{\text{Sending}})$  or  $(P, Q_{\text{Receiving}})$ , that is the device can independently control the active and reactive power at either end of the transmission line. In addition, for a given  $(P, Q)$  control point, it can keep such a point unchanged as the phase-angle varies, that is, it has phase-shifting capabilities, or as the voltage  $V$  varies, that is it also has tap-changer capabilities. Altogether, these capabilities are comparable to that of the dc-link UPFC.

In this paper, the  $\Gamma$ -controller is employed for controlling the complex power flow along the transmission line where such device is connected, through managing the ac voltage with controllable magnitude and phase angle injected into the line.

## 1.2 PWM-series compensator

The series compensators exploit the concept of a variable series reactance. The series reactance is adjusted automatically to satisfy a specified amount of active power flow through the transmission line. The PWM series compensator (PWMSC) is schematised in Fig. 4 [22]. It consists of SIT, compensation capacitors  $C$  and PWM switches  $S$  and  $S'$ .  $D_s$  is the converter's duty ratio defined as the ratio of the on-period of switches  $S'$ , with respect to the total switching period.

The PWMSC consists of: (a) SITs  $T_a$ ,  $T_b$  and  $T_c$ ; (b) compensation capacitors  $C_a$ ,  $C_b$  and  $C_c$  and (c) PWM switches  $S_a$ ,  $S_b$ ,  $S_c$ ,  $S'_a$ ,  $S'_b$  and  $S'_c$ .  $L_a$ ,  $L_b$  and  $L_c$  constitute the transmission line's inductance, including any lumped leakage inductance of the coupling transformer. These inductances are also effective in limiting the ripple in the line current injected by the PWM process. The switches  $S_a$ ,  $S_b$  and  $S_c$  are closed when switches  $S'_a$ ,  $S'_b$  and  $S'_c$  are open and vice-versa.

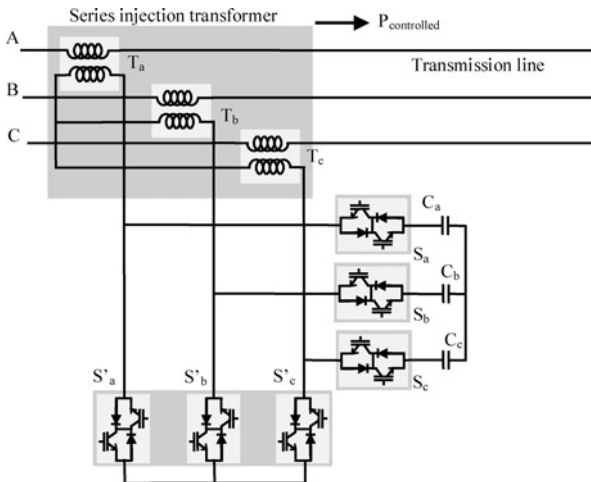


**Fig. 4** Transmission line with PWMSC

During the period when the switches  $S_a$ ,  $S_b$ ,  $S_c$ , are closed, the compensation capacitors are effectively connected in series with the line, reflected through the coupling transformers. During the complementary switching period, the transformer terminals are shorted by the switches  $S'_a$ ,  $S'_b$  and  $S'_c$ , thereby isolating the compensation capacitors from the line.

The equivalent impedance ( $x_{eq}$ ) between the sending and receiving end of the transmission line may be derived using state-space averaging techniques [22] as

$$x_{eq} = x_L - n^2(1 - D_s)^2 x_c \quad (10)$$

where  $x_c$  is the reactance of the capacitors  $C_a$ ,  $C_b$  or  $C_c$ ,  $n$  is the turns ratio of the transformer, and  $x_L$  is the reactance of the inductors  $L_a$ ,  $L_b$  or  $L_c$  (which include the leakage reactance of the coupling transformers  $T_a$ ,  $T_b$  or  $T_c$ , respectively).

The following sections present the incorporation of the  $\Gamma$ -controller and PWMSC into the Newton – Raphson load flow algorithm. The corresponding state variables are incorporated inside the Jacobian and mismatch equations, leading to robust iterative solutions [23]. The proposition has been tested extensively in a wide range of power networks of varying size and degree of operational complexity. In this paper, solution details are provided for a network available in the open literature [24].

## 2 $\Gamma$ -Controller at steady state

The main objective of this section is to include the  $\Gamma$ -controller into a power flow formulation by Newton – Raphson. According to Fig. 5 [18], such device is connected to the transmission line to regulate the complex power flow  $S_{\text{controlled}} = P_{\text{cont}} + jQ_{\text{cont}}$ ; their corresponding equations are required within the formulation.

It is assumed that the shunt phase-shifter and SITs are ideal and have a unity transformation ratio. Besides, it is assumed that the reactive power injection at the fundamental frequency due to the bank FC is negligible [18].

By the transformation ratio

$$\frac{v_s}{v_{\text{series}}} = \frac{1}{D} \quad (11)$$

and from the power conservation

$$v_{\text{series}} i_{\text{series}}^* + v_s i_s^* = 0 \quad (12)$$

where  $v_s$  ( $v_{\text{series}}$ ) is the  $\Gamma$ -controller's shunt (series) voltage  $i_s$  ( $i_{\text{series}}$ ) is the shunt (series) current of the  $\Gamma$ -controller;  $v_s$  and  $v_r$  are the sending and receiving voltages;  $r_{ij}$ ,  $x_{ij}$ ,  $y'_{ij}$  are the parameters of the transmission line (series impedance and shunt admittance).

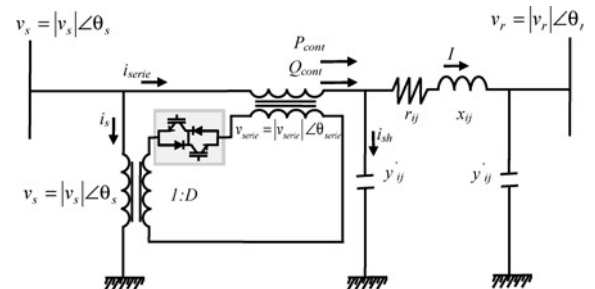


**Fig. 5** Transmission line with a  $\Gamma$ -controller

The current flowing through the series branch becomes

$$i_{\text{series}} = \frac{v_s - v_{\text{series}} - v_r}{z_{ij}} + y'_{ij}(v_s - v_{\text{series}}) \quad (13)$$

$$z_{ij} = r_{ij} + jx_{ij} \quad (14)$$

so that, the sending complex power is

$$S_s = v_s[i_{\text{series}} + i_s]^* = v_s[i_{\text{series}} - D^*i_{\text{series}}]^* \quad (15)$$

Substituting  $i_{\text{series}}$  from (13) into (15) and simplifying

$$S_s = v_s \left( \frac{v_s - v_r}{z_{ij}} + y'_{ij}v_s \right)^* + (-D - D^* + |D|^2) \times \left( \frac{1}{z_{ij}} + y'_{ij} \right)^* |v_s|^2 + D \left( \frac{1}{z_{ij}} \right)^* v_s v_r^* \quad (16)$$

In (16) the first term on the right hand side is already included in the  $s$ -bus power injections of a conventional power flow formulation; the second and third ones must be added into the new formulation as an additional term

$$S_{ad_s} = P_{ad_s} + jQ_{ad_s} = (-D - D^* + |D|^2) \times \left( \frac{1}{z_{ij}} + y'_{ij} \right)^* |v_s|^2 + D \left( \frac{1}{z_{ij}} \right)^* v_s v_r^* \quad (17)$$

The following constants are defined

$$A_{ij} = \text{real} \left\{ \frac{1}{z_{ij}} + y'_{ij} \right\}^*; \quad B_{ij} = \text{imag} \left\{ \frac{1}{z_{ij}} + y'_{ij} \right\}^* \quad (18)$$

$$C_{ij} = \text{real} \left\{ \frac{1}{z_{ij}} \right\}^*; \quad D_{ij} = \text{imag} \left\{ \frac{1}{z_{ij}} \right\}^* \quad (19)$$

In this proposition,  $d_{13}$  and  $d_{24}$  become two new variables that, with the voltages, represent the unknowns in the power flow formulation.

Substituting (8), (18) and (19) into (17) and simplifying

$$S_{ad_s} = (-2d_{13} + d_{13}^2 + d_{24}^2)A_{ij}|v_s|^2 + j(-2d_{13} + d_{13}^2 + d_{24}^2)B_{ij}|v_s|^2 + (d_{13}C_{ij} - d_{24}D_{ij})|v_s||v_r| \cos(\theta_s - \theta_r) + \dots + j(d_{13}C_{ij} - d_{24}D_{ij})|v_s||v_r| \sin(\theta_s - \theta_r) - (d_{24}C_{ij} + d_{13}D_{ij})|v_s||v_r| \sin(\theta_s - \theta_r) + \dots + j(d_{24}C_{ij} + d_{13}D_{ij})|v_s||v_r| \cos(\theta_s - \theta_r) \quad (20)$$

By a similar analysis, the receiving complex power becomes

$$S_r = v_r \left( \frac{v_r - v_s}{z_{ij}} + y'_{ij}v_r \right)^* + v_r \left( \frac{v_{\text{series}}}{z_{ij}} \right)^* \quad (21)$$

In (21) the first term on the right hand side is already included in the conventional Newton–Raphson's power flow algorithm; the second term must be added in the new one

$$S_{ad_r} = v_r v_{\text{series}}^* \left( \frac{1}{z_{ij}} \right)^* \quad (22)$$

Substituting (11) and (19) into (22) and reducing

$$S_{ad_r} = d_{13}C_{ij}|v_s||v_r| \cos(\theta_r - \theta_s) + d_{24}D_{ij}|v_s||v_r| \cos(\theta_r - \theta_s) + jd_{13}D_{ij}|v_s||v_r| \cos(\theta_r - \theta_s) - jd_{24}C_{ij}|v_s||v_r| \cos(\theta_r - \theta_s) + \dots + jd_{13}C_{ij}|v_s||v_r| \sin(\theta_r - \theta_s) - d_{13}D_{ij}|v_s||v_r| \sin(\theta_r - \theta_s) + d_{24}C_{ij}|v_s||v_r| \sin(\theta_r - \theta_s) + jd_{24}D_{ij}|v_s||v_r| \sin(\theta_r - \theta_s) \quad (23)$$

Equations (20) and (23) are used to adjust the complex powers at the sending and receiving buses, respectively.

## 2.1 Controlled power

The controlled complex power may be computed by

$$S_{\text{cont}} = (v_s - v_{\text{series}})i_{\text{series}}^* = P_{\text{cont}} + jQ_{\text{cont}} \quad (24)$$

Substituting  $v_{\text{series}}$  and  $i_{\text{series}}$  from (11) and (13), respectively, and reducing

$$S_{\text{cont}} = (v_s - Dv_s) \left[ \left( \frac{1}{z_{ij}} + y'_{ij} \right) (v_s - Dv_s) - \left( \frac{1}{z_{ij}} \right) v_r \right]^* \quad (25)$$

Using (8), (18) and (19) in (25)

$$S_{\text{cont}} = A_{ij}(1 - 2d_{13} + d_{13}^2 + d_{24}^2)|v_s|^2 + jB_{ij}(1 - 2d_{13} + d_{13}^2 + d_{24}^2)|v_s|^2 - [C_{ij}(1 - d_{13}) + D_{ij}d_{24}]|v_s||v_r| \cos(\theta_s - \theta_r) - j[D_{ij}(1 - d_{13}) - C_{ij}d_{24}]|v_s||v_r| \cos(\theta_s - \theta_r) - j[C_{ij}(1 - d_{13}) + D_{ij}d_{24}]|v_s||v_r| \sin(\theta_s - \theta_r) + [D_{ij}(1 - d_{13}) - C_{ij}d_{24}]|v_s||v_r| \sin(\theta_s - \theta_r) \quad (26)$$

Thus, the active and the reactive controlled power become, respectively

$$P_{\text{cont}} = A_{ij}(1 - 2d_{13} + d_{13}^2 + d_{24}^2)|v_s|^2 - [C_{ij}(1 - d_{13}) + D_{ij}d_{24}]|v_s||v_r| \times \cos(\theta_s - \theta_r) + [D_{ij}(1 - d_{13}) - d_{24}C_{ij}]|v_s||v_r| \sin(\theta_s - \theta_r) \quad (27)$$

$$Q_{\text{cont}} = B_{ij}(1 - 2d_{13} + d_{13}^2 + d_{24}^2)|v_s|^2 - [D_{ij}(1 - d_{13}) - C_{ij}d_{24}]|v_s||v_r| \times \cos(\theta_s - \theta_r) - [C_{ij}(1 - d_{13}) + d_{24}D_{ij}]|v_s||v_r| \sin(\theta_s - \theta_r) \quad (28)$$

Equations (27) and (28) are employed for evaluating the additional unknowns ( $d_{13}$  and  $d_{24}$ ) in the Newton–Raphson load flow algorithm.



Thus, the new Jacobian matrix has a structure as follows

$$J = \begin{bmatrix} J_{\text{conv}} & J_I \\ J_{II} & J_{III} \end{bmatrix} \quad (29)$$

where  $J_{\text{conv}}$  is the conventional Jacobian matrix plus corrections from (16) and (21)  $J_I$ ,  $J_{II}$ , and  $J_{III}$  are sub-matrices formed by the first partial derivatives from expressions (20), (23), (27) and (28), (Appendix A).

$$J_{\text{conv}} = \begin{bmatrix} \frac{\partial P}{\partial \theta} & \frac{\partial P}{\partial |V|} \\ \frac{\partial Q}{\partial \theta} & \frac{\partial Q}{\partial |V|} \end{bmatrix} \quad (30)$$

$$J_I = \begin{bmatrix} \frac{\partial P}{\partial d_{13}} & \frac{\partial P}{\partial d_{24}} \\ \frac{\partial Q}{\partial d_{13}} & \frac{\partial Q}{\partial d_{24}} \end{bmatrix} \quad (31)$$

$$J_{II} = \begin{bmatrix} \frac{\partial P_{\text{cont}}}{\partial \theta} & \frac{\partial P_{\text{cont}}}{\partial |V|} \\ \frac{\partial Q_{\text{cont}}}{\partial \theta} & \frac{\partial Q_{\text{cont}}}{\partial |V|} \end{bmatrix} \quad (32)$$

$$J_{III} = \begin{bmatrix} \frac{\partial P_{\text{cont}}}{\partial d_{13}} & \frac{\partial P_{\text{cont}}}{\partial d_{24}} \\ \frac{\partial Q_{\text{cont}}}{\partial d_{13}} & \frac{\partial Q_{\text{cont}}}{\partial d_{24}} \end{bmatrix} \quad (33)$$

$$x = [\theta |V| d_{13} d_{24}]^T \quad (34)$$

where  $P$ ,  $Q$  are the active and reactive power injection vectors, from the conventional formulation;  $\theta$ ,  $|V|$  are the phase angle and voltage magnitude vectors;  $P_{\text{cont}}$ ,  $Q_{\text{cont}}$  are the controlled active and reactive powers, (27) and (28);  $d_{13}$  and  $d_{24}$  are the difference of duty ratios defined in (8);  $x$  is the state vector.

## 2.2 Example with the $\Gamma$ -controller

The 10-machine power system is used [24] Fig. 6. In order to exemplify the  $\Gamma$ -controller possibilities for controlling the complex power flow, three cases are considered:

1. Nominal case. Power system without FACTS device.
2. Case 1. FACTS device connected in line 26–29, with the purpose of controlling the complex power flow  $S_{26-29} = -2.24 - j0.447$  pu.
3. Case 2. FACTS device connected in line 13–38, with the purpose of controlling the complex power flow  $S_{13-38} = -0.61 + j0.481$  pu.

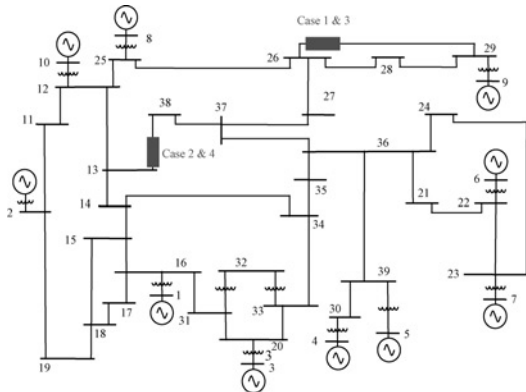


Fig. 6 10-Machine power system

Table 1: Complex voltages with the  $\Gamma$ -controller

Bus	Nominal case	Case 1	Case 2
10	1.047∠ − 4.007°	1.047∠ − 4.009°	1.047∠ − 4.010°
11	1.035∠ − 9.320°	1.035∠ − 9.322°	1.034∠ − 9.268°
12	1.016∠ − 6.443°	1.017∠ − 6.448°	1.015∠ − 6.363°
13	0.985∠ − 9.440°	0.986∠ − 9.443°	0.982∠ − 9.282°
14	0.949∠ − 10.372°	0.950∠ − 10.373°	0.948∠ − 10.352°
15	0.950∠ − 9.119°	0.950∠ − 9.119°	0.950∠ − 9.115°
16	0.952∠ − 8.346°	0.952∠ − 8.347°	0.951∠ − 8.345°
17	0.944∠ − 10.803°	0.944∠ − 10.802°	0.944∠ − 10.800°
18	0.945∠ − 11.366°	0.944∠ − 11.365°	0.942∠ − 11.361°
21	0.985∠ − 4.340°	0.985∠ − 4.347°	0.986∠ − 4.605°
22	1.015∠ 0.190°	1.015∠ 0.1817°	1.015∠ − 0.0799°
23	1.012∠ − 0.081°	1.012∠ − 0.090°	1.012∠ − 0.3521°
24	0.973∠ − 6.801°	0.974∠ − 6.807°	0.974∠ − 7.061°
25	1.026∠ − 4.974°	1.026∠ − 4.990°	1.025∠ − 4.965°
26	1.012∠ − 6.208°	1.014∠ − 6.232°	1.013∠ − 6.361°
27	0.992∠ − 8.329°	0.993∠ − 8.340°	0.993∠ − 8.553°
28	1.016∠ − 2.468°	1.015∠ − 3.400°	1.016∠ − 2.623°
29	1.018∠ 0.467°	1.016∠ − 0.753°	1.019∠ 0.301°
34	0.955∠ − 8.216°	0.955∠ − 8.218°	0.954∠ − 8.260°
35	0.957∠ − 8.535°	0.957∠ − 8.538°	0.957∠ − 8.726°
36	0.973∠ − 6.892°	0.974∠ − 6.897°	0.975∠ − 7.151°
37	0.981∠ − 8.101°	0.982∠ − 8.108°	0.984∠ − 8.418°
38	0.981∠ − 9.086°	0.982∠ − 9.090°	0.986∠ − 9.496°
39	0.984∠ − 1.019°	0.984∠ − 1.021°	0.983∠ − 1.013°

Both the quantities and the location of the device have been elected arbitrarily.

Table 1 exhibits the resulting voltages in the neighbourhood where the device is connected; the first column corresponds to the nominal case [24]. Convergence has been obtained after six iterations with a voltage's tolerance equal to  $1 \times 10^{-5}$ . It is observed that the number of iterations strongly depend on the unknowns  $d_{13}$  and  $d_{24}$  starting points. For the Case 1, Fig. 7 depicts typical initial values of  $d_{13}$  and  $d_{24}$  and the number of iterations for convergence. The corresponding new variables become

$$\text{Case 1: } d_{13} = 0.0170, \quad d_{24} = 0.0424$$

$$\text{Case 2: } d_{13} = -0.0111, \quad d_{24} = 0.0128$$

Solving (8) and (9), which constitute an algebraic set of equations with infinity solutions, for the duty ratios  $d_i$ , result in the PWM values.

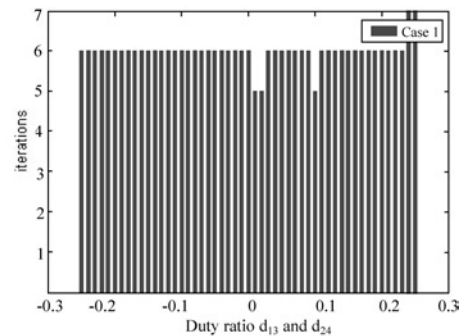


Fig. 7 Initial values against number of iterations (Case 1)

**Table 2: Power flows (Case 1)**

From bus	To bus	Power flow Nominal case	Power flow Case 1
37	27	0.178 – 0.758i	0.1801 – 0.8041i
37	38	2.005 – 0.226i	2.0050 – 0.2147i
36	37	2.188 – 1.058i	2.1894 – 1.0923i
28	29	–3.476 + 0.123i	–3.1301 + 0.1710i
26	29	–1.899 – 0.345i	–2.2400 – 0.4470i
26	28	–1.408 – 0.311i	–1.0654 – 0.3044i
26	27	2.643 + 1.087i	2.6422 + 1.1342i
26	25	–0.726 – 0.600i	–0.7268 – 0.5529i
29	9	–8.247 + 0.428i	–8.2473 + 0.2970i

**Table 3: Power flows (Case 2)**

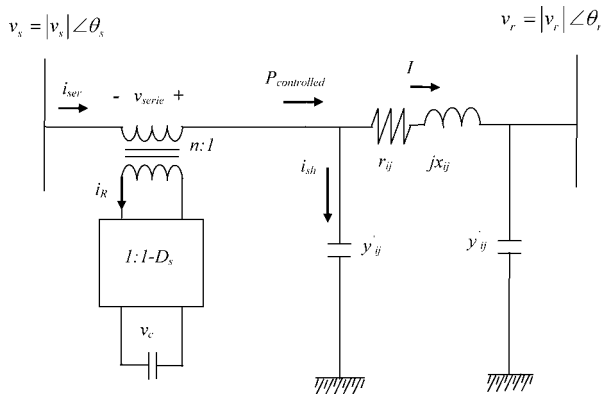
From bus	To bus	Power flow Nominal case	Power flow Case 2
37	27	0.178 – 0.758i	0.0940 – 0.6867i
37	38	2.005 – 0.226i	2.1944 – 0.4668i
36	37	2.188 – 1.058i	2.2932 – 1.2206i
13	38	–0.422 + 0.2311i	–0.6100 + 0.4810i
13	14	0.812 + 0.8278i	0.9090 + 1.3967i
14	15	–1.539 – 0.0015i	–1.5196 – 0.0392i
14	34	–2.652 – 0.202i	–2.5756 – 0.2657i
12	13	3.631 + 1.741i	3.5399 + 1.8880i
12	25	–2.371 + 0.827i	–2.2901 + 0.7394i
11	12	1.234 + 0.2250i	–1.2439 + 0.2401i
12	10	–2.50 – 1.6800i	–2.5000 – 1.7268i

Tables 2 and 3 exhibit complex power flow for both cases on some lines in the surroundings where the device is connected.

As can be noticed, both Case 1 (line 26–29) and Case 2 (line 13–38) the objective is satisfied. This corroborates that the  $\Gamma$ -controller is able to regulate the complex power flow.

### 3 PWMSC at steady state

The aim of this section is to include the PWMSC into the Newton–Raphson power flow formulation. The device is connected in the transmission line as shown in Fig. 4 to regulate the active power flow,  $P_{\text{controlled}}$ , through the

**Fig. 8** Currents in the grid

transmission line, so that the  $P_{\text{controlled}}$  equation is required for evaluating the duty ratio  $D_s$ . Fig. 8 displays the currents in the grid. The insertion of the PWMSC is accounted for at the sending end of the transmission line.

The transformation ratio,  $n$ , is [22]

$$i_R = n \cdot i_{\text{ser}} \quad (35)$$

The capacitor voltage  $v_c$  is the product of its reactance  $x_c$ , the current injection  $i_R$  and the operating duty ratio  $D_s$

$$v_c = n(1 - D_s)i_c x_c \quad (36)$$

The voltage injected in series with the transmission line due to the voltage on the primary of the coupling transformer may be calculated by [22]

$$v_{\text{serie}} = n^2(1 - D_s)^2 x_c i_{\text{ser}} \quad (37)$$

The current flowing through the series branch becomes

$$i_{\text{ser}} = \frac{v_s + v_{\text{serie}} - v_r}{z_{ij}} + y'_{ij}(v_s + v_{\text{serie}}) \quad (38)$$

so that, the sending power results

$$S_s = v_s(i_{\text{ser}})^* \quad (39)$$

Substituting  $i_{\text{ser}}$  from (38) and simplifying

$$S_s = v_s \left( \frac{v_s - v_r}{z_{ij}} + y'_{ij}v_s \right)^* + v_s \left( \frac{v_{\text{serie}}}{z_{ij}} + y'_{ij}v_{\text{serie}} \right)^* \quad (40)$$

In (40) the first term on the right hand side is already included into the  $s$  bus power injections on a conventional power flow formulation. The second one must be added into the new one.

$$S_{ad_s} = P_{ad_s} + jQ_{ad_s} = v_s \left( \frac{v_{\text{serie}}}{z_{ij}} + y'_{ij}v_{\text{serie}} \right)^* \quad (41)$$

Substituting  $v_{\text{serie}}$  from (37) into (38) and simplifying

$$i_{\text{ser}} = \frac{k_1 + j(k_2 + E_{ij}x_{\text{serie}})}{\text{Den}} v_s - \frac{k_3 + F_{ij}x_{\text{serie}} + j(k_4 + G_{ij}x_{\text{serie}})}{\text{Den}} v_r \quad (42)$$

The following constants are defined

$$k_1 = \text{real} \left\{ \frac{1}{z_{ij}} + y'_{ij} \right\}; \quad k_2 = \text{imag} \left\{ \frac{1}{z_{ij}} + y'_{ij} \right\} \quad (43)$$

$$k_3 = \text{real} \left\{ \frac{1}{z_{ij}} \right\}; \quad k_4 = \text{imag} \left\{ \frac{1}{z_{ij}} \right\} \quad (44)$$

$$E_{ij} = k_1^2 + k_2^2 \quad (45)$$

$$F_{ij} = k_2 k_3 - k_1 k_4 \quad (46)$$

$$G_{ij} = k_1 k_3 + k_2 k_4 \quad (47)$$

$$x_{\text{serie}} = n^2(1 - D_s)^2 x_c \quad (48)$$

$$\text{Den} = 1 + 2k_2 x_{\text{serie}} + E_{ij} x_{\text{serie}}^2 \quad (49)$$

Equation (41) should be in function of voltages and angles; thus, substituting  $v_{\text{series}}$  and  $i_{\text{ser}}$  from (37) and (42), respectively, becomes

$$S_{ad_s} = \frac{H_{ij}x_{\text{series}} - A_{ij}E_{ij}x_{\text{series}}^2 - j(I_{ij}x_{\text{series}} + B_{ij}E_{ij}x_{\text{series}}^2)}{\text{Den}} \times |v_s|^2 - \frac{J_{ij}x_{\text{series}} + K_{ij}x_{\text{series}}^2}{\text{Den}} |v_s||v_r| \times \cos(\theta_s - \theta_r) - \dots - j \left( \frac{J_{ij}x_{\text{series}} + K_{ij}x_{\text{series}}^2}{\text{Den}} \right) |v_s||v_r| \times \sin(\theta_s - \theta_r) + j \left( \frac{L_{ij}x_{\text{series}} + M_{ij}x_{\text{series}}^2}{\text{Den}} \right) \times |v_s||v_r| \cos(\theta_s - \theta_r) - \dots - \frac{L_{ij}x_{\text{series}} + M_{ij}x_{\text{series}}^2}{\text{Den}} |v_s||v_r| \sin(\theta_s - \theta_r) \quad (50)$$

where

$$H_{ij} = k_1 B_{ij} - k_2 A_{ij} \quad (51)$$

$$I_{ij} = k_1 A_{ij} + k_2 B_{ij} \quad (52)$$

$$J_{ij} = k_3 B_{ij} - k_4 A_{ij} \quad (53)$$

$$K_{ij} = F_{ij} B_{ij} - G_{ij} A_{ij} \quad (54)$$

$$L_{ij} = k_3 A_{ij} + k_4 B_{ij} \quad (55)$$

$$M_{ij} = F_{ij} A_{ij} + G_{ij} B_{ij} \quad (56)$$

Making a similar analysis, the receiving complex power becomes,

$$S_r = v_r \left( \frac{v_r - v_s}{z_{ij}} + y'_{ij} v_r \right)^* - v_r \left( \frac{v_{\text{series}}}{z_{ij}} \right)^* \quad (57)$$

In (57) the first term on the right hand side is already included in a conventional steady state formulation; the second one must be added into the new formulation.

$$S_{ad_r} = P_{ad_r} + jQ_{ad_r} = -v_r v_{\text{series}}^* \left( \frac{1}{z_{ij}} \right)^* \quad (58)$$

Using (37) into (58) and reducing

$$S_{ad_r} = \frac{(D_{ij}k_1 - C_{ij}k_2)x_{\text{series}} - C_{ij}E_{ij}x_{\text{series}}^2}{\text{Den}} \times |v_s||v_r| \cos(\theta_r - \theta_s) + j \frac{(D_{ij}k_1 - C_{ij}k_2)x_{\text{series}} - C_{ij}E_{ij}x_{\text{series}}^2}{\text{Den}} \times |v_s||v_r| \sin(\theta_r - \theta_s) + \dots + \frac{(C_{ij}k_1 + D_{ij}k_2)x_{\text{series}} + D_{ij}E_{ij}x_{\text{series}}^2}{\text{Den}} \times |v_s||v_r| \sin(\theta_r - \theta_s) - j \frac{(C_{ij}k_1 + D_{ij}k_2)x_{\text{series}} + D_{ij}E_{ij}x_{\text{series}}^2}{\text{Den}} \times |v_s||v_r| \cos(\theta_r - \theta_s) + \dots$$

$$+ \frac{(C_{ij}k_4 - D_{ij}k_3)x_{\text{series}} + (C_{ij}G_{ij} - D_{ij}F_{ij})x_{\text{series}}^2}{\text{Den}} |v_r|^2 + j \frac{(C_{ij}k_3 + D_{ij}k_4)x_{\text{series}} + (C_{ij}F_{ij} + D_{ij}G_{ij})x_{\text{series}}^2}{\text{Den}} |v_r|^2 \quad (59)$$

Equations (50) and (59) are used to adjust the elements of the Jacobian matrix in the sending and receiving buses, respectively.

### 3.1 Controlled power

The controlled active power may be computed as

$$P_{\text{controlled}} = \text{real}[(v_s + v_{\text{series}})i_{\text{ser}}^*] \quad (60)$$

Substituting  $i_{\text{ser}}$  from (42), and reducing

$$P_{\text{controlled}} = \frac{k_1}{\text{Den}} |v_s|^2 - \frac{k_3 + F_{ij}x_{\text{series}}}{\text{Den}} |v_s||v_r| \cos(\theta_s - \theta_r) - \frac{k_4 + G_{ij}x_{\text{series}}}{\text{Den}} |v_s||v_r| \sin(\theta_s - \theta_r) \quad (61)$$

When the PWMSC is added to the power flow formulation,  $D_s$  is an unknown variable, and (61) can be used as the new equation that is added to the set of the conventional ones. Thus, the modified Jacobian matrix exhibits the following structure

$$J = \begin{bmatrix} J_{\text{conv}} & j_I \\ J_{\text{II}} & j_{\text{III}} \end{bmatrix} \quad (62)$$

where  $J_{\text{conv}}$  is the conventional Jacobian matrix plus corrections from (40) and (57);  $j_I$  is a vector formed by the first partial derivatives from (50) and (59) respect  $D_s$ ;  $j_{\text{II}}$  is a vector formed by the first partial derivatives from (61) and  $j_{\text{III}}$  is a scalar evaluated through the first partial derivative respect  $D_s$  of (61) (Appendix B).

In the following expressions  $P$  and  $Q$  are the conventional power injections;  $\theta$  is the phase angle vector  $|v|$  is the voltage magnitude vector  $D_s$  is the duty cycle and  $x$  the state vector, so that the Jacobian is constituted by the following submatrices.

$$J_{\text{conv}} = \begin{bmatrix} \frac{\partial P}{\partial \theta} & \frac{\partial P}{\partial |v|} \\ \frac{\partial Q}{\partial \theta} & \frac{\partial Q}{\partial |v|} \end{bmatrix} \quad (63)$$

$$j_I = \begin{bmatrix} \frac{\partial P_{ad_{s-r}}}{\partial D_s} \\ \frac{\partial Q_{ad_{s-r}}}{\partial D_s} \end{bmatrix} \quad (64)$$

$$j_{\text{II}} = \begin{bmatrix} \frac{\partial P_{\text{controlled}}}{\partial \theta} & \frac{\partial P_{\text{controlled}}}{\partial |v|} \end{bmatrix} \quad (65)$$

$$j_{\text{III}} = \left[ \frac{\partial P_{\text{controlled}}}{\partial D_s} \right] \quad (66)$$

$$x = [\theta \quad |v| \quad D_s]^T \quad (67)$$



### 3.2 Example with PWMSC

The 10-machine power system is employed [24] Fig. 6. In order to exemplify the PWMSC possibilities, two cases are considered:

1. Nominal case. Power system without FACTS device.
2. Case 3. PWMSC device inserted into line 26–29, with the purpose of controlling the active power flow  $P_{26-29} = -2.24$  pu.
3. Case 4. PWMSC device inserted into line 13–38, with the purpose of controlling the active power flow  $P_{13-38} = -0.61$  pu.

Both the controlled quantities and the location of the device have been elected arbitrarily.

Table 4 exhibits the voltages in the surrounding buses where the device is connected; the second column corresponds to the base case [24]. Convergence has been obtained after six iterations with a tolerance of voltage equal to  $1 \times 10^{-5}$ . The corresponding new variable becomes

$$\text{Case 3: } D_s = 0.7916 \text{ pu, } x_{\text{serie}} = 0.0065 \text{ pu}$$

$$\text{Case 4: } D_s = 0.8542 \text{ pu, } x_{\text{serie}} = 0.0032 \text{ pu}$$

Tables 5 and 6 exhibit the complex power flow on some lines in the surroundings where the device is inserted for Case 3 and Case 4.

It can be verified that in both Case 3 (line 26–29) and Case 4 (line 13–38) the objective is satisfactorily satisfied. This corroborates that the PWMSC is able to regulate the active power flow.

**Table 4: Complex voltages**

Bus	Nominal case	Case 3	Case 4
10	1.047∠ − 4.007°	1.047∠ − 2.703°	1.047∠ − 3.251°
11	1.035∠ − 9.320°	1.034∠ − 8.194°	1.034∠ − 8.662°
12	1.016∠ − 6.443°	1.016∠ − 5.139°	1.016∠ − 5.688°
13	0.985∠ − 9.440°	0.985∠ − 8.244°	0.984∠ − 8.658°
14	0.949∠ − 10.372°	0.949∠ − 9.455°	0.949∠ − 9.797°
15	0.950∠ − 9.119°	0.950∠ − 8.386°	0.950∠ − 8.666°
16	0.952∠ − 8.346°	0.952∠ − 7.654°	0.951∠ − 7.918°
17	0.944∠ − 10.803°	0.944∠ − 10.07°	0.943∠ − 10.356°
18	0.945∠ − 11.366°	0.945∠ − 10.619°	0.944∠ − 10.909°
21	0.985∠ − 4.340°	0.985∠ − 3.107°	0.984∠ − 3.6024°
22	1.015∠ 0.190°	1.015∠ 1.423°	1.015∠ 0.9311°
23	1.012∠ − 0.081°	1.012∠ 1.151°	1.011∠ 0.6585°
24	0.973∠ − 6.801°	0.973∠ − 5.568°	0.972∠ − 6.066°
25	1.026∠ − 4.974°	1.026∠ − 3.558°	1.025∠ − 4.220°
26	1.012∠ − 6.208°	1.012∠ − 4.425°	1.011∠ − 5.442°
27	0.992∠ − 8.329°	0.991∠ − 6.756°	0.991∠ − 7.559°
28	1.016∠ − 2.468°	1.016∠ − 0.379°	1.016∠ − 1.699°
29	1.018∠ 0.467°	1.019∠ − 2.379°	1.018∠ 1.227°
34	0.955∠ − 8.216°	0.954∠ − 7.288°	0.954∠ − 7.644°
35	0.957∠ − 8.535°	0.956∠ − 7.393°	0.956∠ − 7.849°
36	0.973∠ − 6.892°	0.973∠ − 5.658°	0.973∠ − 6.156°
37	0.981∠ − 8.101°	0.981∠ − 6.784°	0.980∠ − 7.321°
38	0.981∠ − 9.086°	0.981∠ − 7.815°	0.979∠ − 8.262°
39	0.984∠ − 1.019°	0.984∠ 0.2142°	0.984∠ − 0.2801°

**Table 5: Power flows (Case 3)**

From bus	To bus	Power flow Nominal case	Power flow Case 3
37	27	0.178 − 0.758i	−0.0715 − 0.7431i
37	38	2.005 − 0.226i	2.0999 − 0.2206i
36	37	2.188 − 1.058i	2.0321 − 1.0441i
28	29	− 3.476 + 0.123i	− 3.5922 + 0.1264i
26	29	− 1.899 − 0.345i	− 2.240 − 0.3050i
26	28	− 1.408 − 0.311i	− 1.5224 − 0.2931i
26	27	2.643 + 1.087i	2.8954 + 1.0920i
26	25	− 0.726 − 0.600i	− 0.5230 − 0.6314i
29	9	− 8.247 + 0.428i	− 8.2475 + 0.4563i

**Table 6: Power flows (Case 4)**

From bus	To bus	Power flow Nominal case	Power flow Case 4
37	27	0.178 − 0.758i	0.1861 − 0.7729i
37	38	2.005 − 0.226i	1.9161 − 0.1525i
36	37	2.188 − 1.058i	2.1061 − 1.0034i
13	38	− 0.422 + 0.2311i	− 0.610 + 0.3422i
13	14	0.812 + 0.8278i	0.9664 + 1.4488i
14	15	− 1.539 − 0.0015i	− 1.3905 − 0.0436i
14	34	− 2.652 − 0.202i	− 2.6476 − 0.2144i
12	13	3.631 + 1.741i	3.5975 + 1.8001i
12	25	− 2.371 + 0.827i	− 2.3790 + 0.8126i
11	12	1.234 + 0.2250i	− 1.2750 + 0.2396i
12	10	− 2.50 − 1.6800i	− 2.5000 − 1.7154i

## 4 Conclusions

The direct ac/ac power conversion principle of the matrix converter leads to the distinct structure with no large dc-link energy storage components. Consequently, the matrix converter topology can be implemented with compact size and volume compared with the diode rectifier based PWM-VSC. This paper presents the major expressions that must be included into the power flow formulation based on the Newton–Raphson method for taking into account the novel  $\Gamma$ -controller and the PWMSC. The corresponding state variables are incorporated inside the Jacobian and mismatch equations, leading to robust iterative solutions. Results exhibit the applicability of such device for controlling the complex power flow and the active power flow through a transmission line, respectively.

## 5 Acknowledgment

Juan M. Ramirez and Juan M. González thanks to CONACyT under grant No. 43478.

## 6 References

- 1 Gyugyi, L.: ‘Application characteristics of converter-based FACTS controllers’. Proc. Int. Conf. Power System Technology (PowerCon 2000), December 2000, Piscataway, NJ, USA), vol. 1, pp. 391–396
- 2 IEEE Power Engineering Society/CIGRE: ‘FACTS overview’. Publication 95TP108 (IEEE Press, New York, 1995)
- 3 Hingorani, N.G., and Gyugyi, L.: ‘Understanding FACTS’ (IEEE Press, New York, 1999)

- 4 Song, Y.H., and Johns, A.T. (Eds.): 'Flexible AC transmission systems (FACTS)' (IEE Press, London, 1999)
- 5 IEEE Power Engineering Society: 'FACTS applications', Publication 96TP116-0 (IEEE Press, New York, 1996)
- 6 Nabavi-niaki, A., and Iravani, M.R.: 'Steady-state and dynamic models of unified power flow controller (UPFC) for power system studies'. IEEE/PES Winter Meeting '96 WM 257-6 PWRs, Baltimore, MD, 21–25 January 1996
- 7 Sen, K.K., and Stacey, E.J.: 'UPFC – Unified power flow controller: theory, modeling, and applications', *IEEE Trans. Power Deliv.*, 1998, **13**, (4), pp. 1453–1460
- 8 Gyugyi, L., Schauder, C.D., and Sen, K.K.: 'Static synchronous series compensator: a solid-state approach to the series compensation of transmission lines', *IEEE Trans. Power Deliv.*, 1997, **12**, (1), pp. 406–417
- 9 Gotham, D., and Heydt, G.T.: 'Power flow control and power flow studies for systems with FACTS devices', *IEEE Trans. Power Syst.*, 1998, **13**, (1), pp. 60–65
- 10 Dobson, I.: 'Stability of ideal thyristor and diode switching circuits', *IEEE Trans. Circ. Syst.*, 1995, **42**, (12), pp. 517–529
- 11 Matavelli, P., Verghese, G., and Stankovic, A.M.: 'Phasor dynamics of thyristor – controlled series capacitor systems', *IEEE Trans. Power Syst.*, 1997, **12**, (3), pp. 1259–1267
- 12 Perkins, B.K., and Iravani, M.R.: 'Dynamic modeling of high power static switching circuits in the dq-frame', *IEEE Trans. Power Syst.*, 1999, **14**, (2), pp. 678–684
- 13 Canizares, C.A., and Four, Z.T.: 'Analysis for SVC and TCSC controllers in voltage collapse', *IEEE Trans. Power Syst.*, 1999, **14**, (1), pp. 158–165
- 14 Chen, Y., and Ooi, B.T.: 'STATCOM based on multimodules of multilevel converters under multiple regulation feedback control', *IEEE Trans. Power Electron.*, 1999, **14**, (5), pp. 959–965
- 15 Ooi, B.T., and Dai, S.-Z.: 'Series-type solid-state static VAR compensator', *IEEE Trans. Power Electron.*, 1993, **8**, (2), pp. 164–169
- 16 Ooi, B.T., and Kazerani, M.: 'Voltage-source matrix converter as a controller in flexible AC transmission systems', *IEEE Trans. Power Deliv.*, 1998, **13**, (1), pp. 247–253
- 17 Venkataramanan, G.: 'Three-phase vector switching converters for power flow control', *IEE Proc., Electr. Power Appl.*, 2004, **151**, (3), pp. 321–333
- 18 Mancilla-David, F., and Venkataramanan, G.: 'A pulse width modulated AC link unified power flow controller'. Proc. 2005 IEEE Power Engineering Society General Meeting, San Francisco, CA, USA
- 19 Peng, F.Z., Chen, L., and Zhang, F.: 'Simple topologies of PWM AC-AC converters', *IEEE Power Electron. Lett.*, 2003, **1**, (1), pp. 10–13
- 20 Simon, O., Mahlein, J., Muenzer, M.N., and Bruckmann, M.: 'Modern solutions for industrial matrix-converter applications', *IEEE Trans. Ind. Electron.*, 2002, **49**, (2), pp. 401–406
- 21 Wheeler, P., Clare, J., Empringham, L., Apap, M., and Bland, M.: 'Matrix converters', *Power Eng. J.*, 2002, **16**, (6), pp. 273–282
- 22 Venkataramanan, G., and Johnson, B.K.: 'Pulse width modulated series compensator', *IEE Proc., Gener. Transm. Distrib.*, 2002, **149**, (1), pp. 71–75
- 23 Fuerte-esquivel, C.R., and Acha, E.: 'Unified power flow controller: a critical comparison of newton–Raphson UPFC algorithms in power flow studies', *IEE Proc., Gener. Transm. Distrib.*, 1997, **144**, (5), pp. 437–444
- 24 Padiyar, K.R.: 'Power system dynamics stability and control' (John Wiley & Sons, 1996)
- 25 Wheeler, P., Clare, J., Empringham, L., Apap, M., and Bland, M.: 'Matrix converters', *Power Eng. J.*, 2002, **16**, (6), pp. 273–282
- 26 Venkataramanan, G., and Johnson, B.K.: 'Pulse width modulated series compensator', *IEE Proc., Gener. Transm. Distrib.*, 2002, **149**, (1), pp. 71–75
- 27 Fuerte-Esquivel, C.R., and Acha, E.: 'Unified power flow controller: a critical comparison of Newton–Raphson UPFC algorithms in power flow studies', *IEE Proc., Gener. Transm. Distrib.*, 1997, **144**, (5), pp. 437–444

## 7 Appendix A

Corrections on submatrix  $J_{\text{conv}}$

$$\begin{aligned} \frac{\partial P_{ad_s}}{\partial |v_s|} = & 2(-2d_{13} + d_{13}^2 + d_{24}^2)A_{ij}|v_s| \\ & + (d_{13}C_{ij} - d_{24}D_{ij})|v_r| \cos(\theta_s - \theta_r) \\ & - (d_{24}C_{ij} + d_{13}D_{ij})|v_r| \sin(\theta_s - \theta_r) \end{aligned}$$

$$\begin{aligned} \frac{\partial P_{ad_s}}{\partial \theta_s} = & -(d_{13}C_{ij} - d_{24}D_{ij})|v_s| \\ & \times |v_r| \sin(\theta_s - \theta_r) - (d_{24}C_{ij} + d_{13}D_{ij}) \\ & \times |v_s||v_r| \cos(\theta_s - \theta_r) \end{aligned}$$

$$\begin{aligned} \frac{\partial P_{ad_s}}{\partial |v_r|} = & (d_{13}C_{ij} - d_{24}D_{ij})|v_s| \\ & \times \cos(\theta_s - \theta_r) - (d_{24}C_{ij} + d_{13}D_{ij}) \\ & \times |v_s| \sin(\theta_s - \theta_r) \end{aligned}$$

$$\begin{aligned} \frac{\partial P_{ad_s}}{\partial \theta_r} = & (d_{13}C_{ij} - d_{24}D_{ij})|v_s||v_r| \\ & \times \sin(\theta_s - \theta_r) + (d_{24}C_{ij} + d_{13}D_{ij}) \\ & \times |v_s||v_r| \cos(\theta_s - \theta_r) \end{aligned}$$

$$\begin{aligned} \frac{\partial Q_{ad_s}}{\partial |v_s|} = & 2(-2d_{13} + d_{13}^2 + d_{24}^2)B_{ij}|v_s| \\ & + (d_{13}C_{ij} - d_{24}D_{ij})|v_r| \sin(\theta_s - \theta_r) \\ & + (d_{24}C_{ij} + d_{13}D_{ij})|v_r| \cos(\theta_s - \theta_r) \end{aligned}$$

$$\begin{aligned} \frac{\partial Q_{ad_s}}{\partial \theta_s} = & (d_{13}C_{ij} - d_{24}D_{ij})|v_s||v_r| \\ & \times \cos(\theta_s - \theta_r) - (d_{24}C_{ij} + d_{13}D_{ij}) \\ & \times |v_s||v_r| \sin(\theta_s - \theta_r) \end{aligned}$$

$$\begin{aligned} \frac{\partial Q_{ad_s}}{\partial |v_r|} = & (d_{13}C_{ij} - d_{24}D_{ij})|v_s| \\ & \times \sin(\theta_s - \theta_r) + (d_{24}C_{ij} + d_{13}D_{ij}) \\ & \times |v_s| \cos(\theta_s - \theta_r) \end{aligned}$$

$$\begin{aligned} \frac{\partial Q_{ad_s}}{\partial \theta_r} = & -(d_{13}C_{ij} - d_{24}D_{ij})|v_s||v_r| \\ & \times \cos(\theta_s - \theta_r) + (d_{24}C_{ij} + d_{13}D_{ij}) \\ & \times |v_s||v_r| \sin(\theta_s - \theta_r) \end{aligned}$$

$$\begin{aligned} \frac{\partial P_{ad_r}}{\partial |v_s|} = & C_{ij}d_{13}|v_r| \cos(\theta_r - \theta_s) \\ & - D_{ij}d_{13}|v_r| \sin(\theta_r - \theta_s) \\ & + d_{24}C_{ij}|v_r| \sin(\theta_r - \theta_s) \\ & + d_{24}D_{ij}|v_r| \cos(\theta_r - \theta_s) \end{aligned}$$

$$\begin{aligned} \frac{\partial P_{ad_r}}{\partial \theta_s} = & d_{13}C_{ij}|v_s||v_r| \sin(\theta_r - \theta_s) \\ & + d_{13}D_{ij}|v_s||v_r| \cos(\theta_r - \theta_s) \\ & - d_{24}C_{ij}|v_s||v_r| \cos(\theta_r - \theta_s) \\ & + d_{24}D_{ij}|v_s||v_r| \sin(\theta_r - \theta_s) \end{aligned}$$

$$\begin{aligned}
\frac{\partial P_{ad_r}}{\partial |v_r|} &= C_{ij}d_{13}|v_s| \cos(\theta_r - \theta_s) \\
&\quad - D_{ij}d_{13}|v_s| \sin(\theta_r - \theta_s) \\
&\quad + d_{24}C_{ij}|v_s| \sin(\theta_r - \theta_s) \\
&\quad + d_{24}D_{ij}|v_s| \cos(\theta_r - \theta_s) \\
\frac{\partial P_{ad_r}}{\partial \theta_r} &= -d_{13}C_{ij}|v_s||v_r| \sin(\theta_r - \theta_s) \\
&\quad - d_{13}D_{ij}|v_s||v_r| \cos(\theta_r - \theta_s) \\
&\quad + d_{24}C_{ij}|v_s||v_r| \cos(\theta_r - \theta_s) \\
&\quad - d_{24}D_{ij}|v_s||v_r| \sin(\theta_r - \theta_s) \\
\frac{\partial Q_{ad_r}}{\partial |v_s|} &= d_{13}C_{ij}|v_r| \sin(\theta_r - \theta_s) \\
&\quad + d_{13}D_{ij}|v_r| \cos(\theta_r - \theta_s) \\
&\quad - d_{24}C_{ij}|v_r| \cos(\theta_r - \theta_s) \\
&\quad + d_{24}D_{ij}|v_r| \sin(\theta_r - \theta_s) \\
\frac{\partial Q_{ad_r}}{\partial \theta_s} &= -d_{13}C_{ij}|v_s||v_r| \cos(\theta_r - \theta_s) \\
&\quad + d_{13}D_{ij}|v_s||v_r| \sin(\theta_r - \theta_s) \\
&\quad - d_{24}C_{ij}|v_s||v_r| \sin(\theta_r - \theta_s) \\
&\quad - d_{24}D_{ij}|v_s||v_r| \cos(\theta_r - \theta_s) \\
\frac{\partial Q_{ad_r}}{\partial |v_r|} &= d_{13}C_{ij}|v_s| \sin(\theta_r - \theta_s) \\
&\quad + d_{13}D_{ij}|v_s| \cos(\theta_r - \theta_s) \\
&\quad - d_{24}C_{ij}|v_s| \cos(\theta_r - \theta_s) \\
&\quad + d_{24}D_{ij}|v_s| \sin(\theta_r - \theta_s) \\
\frac{\partial Q_{ad_r}}{\partial \theta_r} &= d_{13}C_{ij}|v_s||v_r| \cos(\theta_r - \theta_s) \\
&\quad - d_{13}D_{ij}|v_s||v_r| \sin(\theta_r - \theta_s) \\
&\quad + d_{24}C_{ij}|v_s||v_r| \sin(\theta_r - \theta_s) \\
&\quad + d_{24}D_{ij}|v_s||v_r| \cos(\theta_r - \theta_s)
\end{aligned}$$

Elements of submatrix  $\mathbf{J}_I$

$$\begin{aligned}
\frac{\partial P_{ad_s}}{\partial d_{13}} &= (2d_{13} - 2)A_{ij}|v_s|^2 \\
&\quad + C_{ij}|v_s||v_r| \cos(\theta_s - \theta_r) \\
&\quad - D_{ij}|v_s||v_r| \sin(\theta_s - \theta_r) \\
\frac{\partial P_{ad_s}}{\partial d_{24}} &= 2d_{24}A_{ij}|v_s|^2 \\
&\quad - D_{ij}|v_s||v_r| \cos(\theta_s - \theta_r) \\
&\quad - C_{ij}|v_s||v_r| \sin(\theta_s - \theta_r) \\
\frac{\partial Q_{ad_s}}{\partial d_{13}} &= (2d_{13} - 2)B_{ij}|v_s|^2 \\
&\quad + C_{ij}|v_s||v_r| \sin(\theta_s - \theta_r) \\
&\quad + D_{ij}|v_s||v_r| \cos(\theta_s - \theta_r)
\end{aligned}$$

$$\begin{aligned}
\frac{\partial Q_{ad_s}}{\partial d_{24}} &= 2d_{24}B_{ij}|v_s|^2 \\
&\quad - D_{ij}|v_s||v_r| \sin(\theta_s - \theta_r) \\
&\quad + C_{ij}|v_s||v_r| \cos(\theta_s - \theta_r)
\end{aligned}$$

$$\begin{aligned}
\frac{\partial P_{ad_r}}{\partial d_{13}} &= C_{ij}|v_s||v_r| \cos(\theta_r - \theta_s) \\
&\quad - D_{ij}|v_s||v_r| \sin(\theta_r - \theta_s)
\end{aligned}$$

$$\begin{aligned}
\frac{\partial P_{ad_r}}{\partial d_{24}} &= C_{ij}|v_s||v_r| \sin(\theta_r - \theta_s) \\
&\quad + D_{ij}|v_s||v_r| \cos(\theta_r - \theta_s)
\end{aligned}$$

$$\begin{aligned}
\frac{\partial Q_{ad_r}}{\partial d_{13}} &= C_{ij}|v_s||v_r| \sin(\theta_r - \theta_s) \\
&\quad + D_{ij}|v_s||v_r| \cos(\theta_r - \theta_s)
\end{aligned}$$

$$\begin{aligned}
\frac{\partial Q_{ad_r}}{\partial d_{24}} &= -C_{ij}|v_s||v_r| \cos(\theta_r - \theta_s) \\
&\quad + D_{ij}|v_s||v_r| \sin(\theta_r - \theta_s)
\end{aligned}$$

Elements of submatrix  $\mathbf{J}_{II}$

$$\begin{aligned}
\frac{\partial P_{\text{cont}}}{\partial |v_r|} &= -[C_{ij}(1 - d_{13}) + D_{ij}d_{24}] \\
&\quad \times |v_s| \cos(\theta_s - \theta_r) \\
&\quad + [D_{ij}(1 - d_{13}) - C_{ij}d_{24}] \\
&\quad \times |v_s||v_r| \sin(\theta_s - \theta_r)
\end{aligned}$$

$$\begin{aligned}
\frac{\partial P_{\text{cont}}}{\partial \theta_s} &= [C_{ij}(1 - d_{13}) + D_{ij}d_{24}] \\
&\quad \times |v_s||v_r| \sin(\theta_s - \theta_r) \\
&\quad + [D_{ij}(1 - d_{13}) - C_{ij}d_{24}] \\
&\quad \times |v_s||v_r| \cos(\theta_s - \theta_r)
\end{aligned}$$

$$\begin{aligned}
\frac{\partial P_{\text{cont}}}{\partial |v_r|} &= -[C_{ij}(1 - d_{13}) + D_{ij}d_{24}] \\
&\quad \times |v_s| \cos(\theta_s - \theta_r) \\
&\quad + [D_{ij}(1 - d_{13}) - C_{ij}d_{24}] \\
&\quad \times |v_s||v_r| \sin(\theta_s - \theta_r)
\end{aligned}$$

$$\begin{aligned}
\frac{\partial P_{\text{cont}}}{\partial \theta_r} &= -[C_{ij}(1 - d_{13}) + D_{ij}d_{24}] \\
&\quad \times |v_s||v_r| \sin(\theta_s - \theta_r) \\
&\quad - [D_{ij}(1 - d_{13}) - C_{ij}d_{24}] \\
&\quad \times |v_s||v_r| \cos(\theta_s - \theta_r)
\end{aligned}$$

$$\begin{aligned}
\frac{\partial Q_{\text{cont}}}{\partial |v_s|} &= 2B_{ij}(1 - 2d_{13} + d_{13}^2 + d_{24}^2)|v_s| \\
&\quad - [D_{ij}(1 - d_{13}) - d_{24}C_{ij}]|v_r| \cos(\theta_s - \theta_r) \\
&\quad - [C_{ij}(1 - d_{13}) + d_{24}D_{ij}]|v_r| \sin(\theta_s - \theta_r)
\end{aligned}$$

$$\begin{aligned}
\frac{\partial Q_{\text{cont}}}{\partial \theta_s} &= [D_{ij}(1 - d_{13}) - C_{ij}d_{24}]|v_s||v_r| \sin(\theta_s - \theta_r) \\
&\quad - [C_{ij}(1 - d_{13}) + D_{ij}d_{24}]|v_s||v_r| \cos(\theta_s - \theta_r) \\
\frac{\partial Q_{\text{cont}}}{\partial |v_r|} &= -[D_{ij}(1 - d_{13}) - C_{ij}d_{24}]|v_s||v_r| \cos(\theta_s - \theta_r) \\
&\quad - [C_{ij}(1 - d_{13}) + D_{ij}d_{24}]|v_s||v_r| \sin(\theta_s - \theta_r) \\
\frac{\partial Q_{\text{cont}}}{\partial \theta_r} &= -[D_{ij}(1 - d_{13}) - C_{ij}d_{24}]|v_s||v_r| \sin(\theta_s - \theta_r) \\
&\quad + [C_{ij}(1 - d_{13}) + D_{ij}d_{24}]|v_s||v_r| \cos(\theta_s - \theta_r)
\end{aligned}$$

Elements of submatrix  $\mathbf{J}_{\text{III}}$

$$\begin{aligned}
\frac{\partial P_{\text{cont}}}{\partial d_{13}} &= A_{ij}(-2 + 2d_{13})|v_s|^2 + C_{ij}|v_s||v_r| \cos(\theta_s - \theta_r) \\
&\quad - D_{ij}|v_s||v_r| \sin(\theta_s - \theta_r) \\
\frac{\partial P_{\text{cont}}}{\partial d_{24}} &= 2A_{ij}d_{24}|v_s|^2 - D_{ij}|v_s||v_r| \cos(\theta_s - \theta_r) \\
&\quad - C_{ij}|v_s||v_r| \sin(\theta_s - \theta_r) \\
\frac{\partial Q_{\text{cont}}}{\partial d_{13}} &= B_{ij}(-2 + 2d_{13})|v_s|^2 + C_{ij}|v_s||v_r| \sin(\theta_s - \theta_r) \\
&\quad + D_{ij}|v_s||v_r| \cos(\theta_s - \theta_r) \\
\frac{\partial Q_{\text{cont}}}{\partial d_{24}} &= 2B_{ij}d_{24}|v_s|^2 - D_{ij}|v_s||v_r| \sin(\theta_s - \theta_r) \\
&\quad + C_{ij}|v_s||v_r| \cos(\theta_s - \theta_r)
\end{aligned}$$

## 8 Appendix B

Corrections on submatrix  $\mathbf{J}_{\text{conv}}$

$$\begin{aligned}
\frac{\partial P_{ad_s}}{\partial |v_s|} &= \frac{2x_{\text{serie}}(H_{ij} - A_{ij}E_{ij}x_{\text{serie}})}{\text{Den}}|v_s| \\
&\quad - \frac{x_{\text{serie}}(J_{ij} + K_{ij}x_{\text{serie}})}{\text{Den}}|v_r| \cos(\theta_s - \theta_r) \\
&\quad - \frac{x_{\text{serie}}(L_{ij} + M_{ij}x_{\text{serie}})}{\text{Den}}|v_r| \sin(\theta_s - \theta_r) \\
\frac{\partial P_{ad_s}}{\partial \theta_s} &= \frac{x_{\text{serie}}(J_{ij} + K_{ij}x_{\text{serie}})}{\text{Den}}|v_s||v_r| \sin(\theta_s - \theta_r) \\
&\quad - \frac{x_{\text{serie}}(L_{ij} + M_{ij}x_{\text{serie}})}{\text{Den}}|v_s||v_r| \cos(\theta_s - \theta_r) \\
\frac{\partial P_{ad_s}}{\partial |v_r|} &= -\frac{x_{\text{serie}}(J_{ij} + K_{ij}x_{\text{serie}})}{\text{Den}}|v_s| \cos(\theta_s - \theta_r) \\
&\quad - \frac{x_{\text{serie}}(L_{ij} + M_{ij}x_{\text{serie}})}{\text{Den}}|v_s| \sin(\theta_s - \theta_r)
\end{aligned}$$

$$\begin{aligned}
\frac{\partial P_{ad_s}}{\partial \theta_r} &= -\frac{x_{\text{serie}}(J_{ij} + K_{ij}x_{\text{serie}})}{\text{Den}}|v_s||v_r| \sin(\theta_s - \theta_r) \\
&\quad + \frac{x_{\text{serie}}(L_{ij} + M_{ij}x_{\text{serie}})}{\text{Den}}|v_s||v_r| \cos(\theta_s - \theta_r) \\
\frac{\partial Q_{ad_s}}{\partial |v_s|} &= -\frac{2x_{\text{serie}}(I_{ij} - B_{ij}E_{ij}x_{\text{serie}})}{\text{Den}}|v_s| \\
&\quad - \frac{x_{\text{serie}}(J_{ij} + K_{ij}x_{\text{serie}})}{\text{Den}}|v_r| \sin(\theta_s - \theta_r) \\
&\quad + \frac{x_{\text{serie}}(L_{ij} + M_{ij}x_{\text{serie}})}{\text{Den}}|v_r| \cos(\theta_s - \theta_r) \\
\frac{\partial Q_{ad_s}}{\partial \theta_s} &= -\frac{x_{\text{serie}}(J_{ij} + K_{ij}x_{\text{serie}})}{\text{Den}}|v_s||v_r| \cos(\theta_s - \theta_r) \\
&\quad - \frac{x_{\text{serie}}(L_{ij} + M_{ij}x_{\text{serie}})}{\text{Den}}|v_s||v_r| \sin(\theta_s - \theta_r) \\
\frac{\partial Q_{ad_s}}{\partial |v_r|} &= -\frac{x_{\text{serie}}(J_{ij} + K_{ij}x_{\text{serie}})}{\text{Den}}|v_s| \sin(\theta_s - \theta_r) \\
&\quad + \frac{x_{\text{serie}}(L_{ij} + M_{ij}x_{\text{serie}})}{\text{Den}}|v_s| \cos(\theta_s - \theta_r) \\
\frac{\partial Q_{ad_s}}{\partial \theta_r} &= \frac{x_{\text{serie}}(J_{ij} + K_{ij}x_{\text{serie}})}{\text{Den}}|v_s||v_r| \cos(\theta_s - \theta_r) \\
&\quad + \frac{x_{\text{serie}}(L_{ij} + M_{ij}x_{\text{serie}})}{\text{Den}}|v_s||v_r| \sin(\theta_s - \theta_r) \\
\frac{\partial P_{ad_r}}{\partial |v_s|} &= \frac{(D_{ij}k_1 - C_{ij}k_2)x_{\text{serie}} - C_{ij}E_{ij}x_{\text{serie}}^2}{\text{Den}} \\
&\quad \times |v_r| \cos(\theta_r - \theta_s) \\
&\quad + \frac{(C_{ij}k_1 + D_{ij}k_2)x_{\text{serie}} + D_{ij}E_{ij}x_{\text{serie}}^2}{\text{Den}} \\
&\quad \times |v_r| \sin(\theta_r - \theta_s) \\
\frac{\partial P_{ad_r}}{\partial \theta_s} &= \frac{(D_{ij}k_1 - C_{ij}k_2)x_{\text{serie}} - C_{ij}E_{ij}x_{\text{serie}}^2}{\text{Den}}|v_s||v_r| \sin(\theta_r - \theta_s) \\
&\quad - \frac{(C_{ij}k_1 + D_{ij}k_2)x_{\text{serie}} + D_{ij}E_{ij}x_{\text{serie}}^2}{\text{Den}} \\
&\quad \times |v_s||v_r| \cos(\theta_r - \theta_s) \\
\frac{\partial P_{ad_r}}{\partial |v_r|} &= \frac{(D_{ij}k_1 - C_{ij}k_2)x_{\text{serie}} - C_{ij}E_{ij}x_{\text{serie}}^2}{\text{Den}} \\
&\quad \times |v_r| \cos(\theta_r - \theta_s) \\
&\quad + \frac{(C_{ij}k_1 + D_{ij}k_2)x_{\text{serie}} + D_{ij}E_{ij}x_{\text{serie}}^2}{\text{Den}} \\
&\quad \times |v_r| \sin(\theta_r - \theta_s) + \dots \\
&\quad + \frac{2(C_{ij}k_4 - D_{ij}k_3)x_{\text{serie}} + 2(C_{ij}G_{ij} - D_{ij}F_{ij})x_{\text{serie}}^2}{\text{Den}}|v_r|
\end{aligned}$$

$$\frac{\partial P_{ad_r}}{\partial \theta_r} = -\frac{(D_{ij}k_1 - C_{ij}k_2)x_{\text{series}} - C_{ij}E_{ij}x_{\text{series}}^2}{\text{Den}}|v_s||v_r|\sin(\theta_r - \theta_s) \\ + \frac{(C_{ij}k_1 + D_{ij}k_2)x_{\text{series}} + D_{ij}E_{ij}x_{\text{series}}^2}{\text{Den}}|v_s||v_r|\cos(\theta_r - \theta_s)$$

$$\frac{\partial Q_{ad_r}}{\partial |v_s|} = \frac{(D_{ij}k_1 - C_{ij}k_2)x_{\text{series}} - C_{ij}E_{ij}x_{\text{series}}^2}{\text{Den}}|v_r|\sin(\theta_r - \theta_s) \\ - \frac{(C_{ij}k_1 + D_{ij}k_2)x_{\text{series}} + D_{ij}E_{ij}x_{\text{series}}^2}{\text{Den}}|v_r|\cos(\theta_r - \theta_s)$$

$$\frac{\partial Q_{ad_r}}{\partial \theta_r} = -\frac{(D_{ij}k_1 - C_{ij}k_2)x_{\text{series}} - C_{ij}E_{ij}x_{\text{series}}^2}{\text{Den}}|v_s||v_r|\cos(\theta_r - \theta_s) \\ - \frac{(C_{ij}k_1 + D_{ij}k_2)x_{\text{series}} + D_{ij}E_{ij}x_{\text{series}}^2}{\text{Den}}|v_s||v_r|\sin(\theta_r - \theta_s)$$

$$\frac{\partial Q_{ad_r}}{\partial |v_r|} = \frac{(D_{ij}k_1 - C_{ij}k_2)x_{\text{series}} - C_{ij}E_{ij}x_{\text{series}}^2}{\text{Den}}|v_s|\sin(\theta_r - \theta_s) \\ - \frac{(C_{ij}k_1 + D_{ij}k_2)x_{\text{series}} + D_{ij}E_{ij}x_{\text{series}}^2}{\text{Den}}|v_s|\cos(\theta_r - \theta_s) + \dots \\ + \frac{2(C_{ij}k_3 + D_{ij}k_4)x_{\text{series}} + 2(C_{ij}F_{ij} + D_{ij}G_{ij})x_{\text{series}}^2}{\text{Den}}|v_r|$$

$$\frac{\partial Q_{ad_r}}{\partial \theta_r} = \frac{(D_{ij}k_1 - C_{ij}k_2)x_{\text{series}} - C_{ij}E_{ij}x_{\text{series}}^2}{\text{Den}}|v_s||v_r|\cos(\theta_r - \theta_s) \\ + \frac{(C_{ij}k_1 + D_{ij}k_2)x_{\text{series}} + D_{ij}E_{ij}x_{\text{series}}^2}{\text{Den}} \\ \times |v_s||v_r|\sin(\theta_r - \theta_s)$$

Elements of submatrix  $j_1$

$$\frac{\partial P_{ad_s}}{\partial D_s} = \frac{2x_c n^2(1 - D_s)[-H_{ij} + 2x_{\text{series}}E_{ij}A_{ij}]}{\text{Den}}|v_s|^2 \\ + \frac{x_{\text{series}}(H_{ij} - E_{ij}A_{ij}x_{\text{series}})}{\text{Den}^2} \\ \times \left\{ 4x_c n^2(1 - D_s)[k_2 + x_{\text{series}}E_{ij}] \right\}|v_s|^2 \\ + \frac{2x_c n^2(1 - D_s)[J_{ij} + 2K_{ij}x_{\text{series}}]}{\text{Den}}|v_s||v_r|\cos(\theta_s - \theta_r) \\ - \frac{x_{\text{series}}[J_{ij} + K_{ij}x_{\text{series}}]\left\{ 4x_c n^2(1 - D_s)[k_2 + x_{\text{series}}E_{ij}] \right\}}{\text{Den}^2} \\ \times |v_s||v_r|\cos(\theta_s - \theta_r) \\ + \frac{2x_c n^2(1 - D_s)[L_{ij} + 2M_{ij}x_{\text{series}}]}{\text{Den}}|v_s||v_r|\sin(\theta_s - \theta_r) \\ - \frac{x_{\text{series}}[L_{ij} + M_{ij}x_{\text{series}}]\left\{ 4x_c n^2(1 - D_s)[k_2 + x_{\text{series}}E_{ij}] \right\}}{\text{Den}^2} \\ \times |v_s||v_r|\sin(\theta_s - \theta_r)$$

$$\frac{\partial Q_{ad_s}}{\partial D_s} = \frac{2x_c n^2(1 - D_s)[I_{ij} + 2x_{\text{series}}E_{ij}B_{ij}]}{\text{Den}}|v_s|^2 \\ + \frac{x_{\text{series}}(I_{ij} - E_{ij}B_{ij}x_{\text{series}})\left\{ 4x_c n^2(1 - D_s)[k_2 + x_{\text{series}}E_{ij}] \right\}}{\text{Den}^2}|v_s|^2 \\ - \frac{2x_c n^2(1 - D_s)[L_{ij} + 2M_{ij}x_{\text{series}}]}{\text{Den}}|v_s||v_r|\cos(\theta_s - \theta_r) \\ + \frac{x_{\text{series}}[L_{ij} + M_{ij}x_{\text{series}}]\left\{ 4x_c n^2(1 - D_s)[k_2 + x_{\text{series}}E_{ij}] \right\}}{\text{Den}^2} \\ \times |v_s||v_r|\cos(\theta_s - \theta_r) \\ + \frac{2x_c n^2(1 - D_s)[J_{ij} + 2K_{ij}x_{\text{series}}]}{\text{Den}}|v_s||v_r|\sin(\theta_s - \theta_r) \\ - \frac{x_{\text{series}}[J_{ij} + K_{ij}x_{\text{series}}]\left\{ 4x_c n^2(1 - D_s)[k_2 + x_{\text{series}}E_{ij}] \right\}}{\text{Den}^2} \\ \times |v_s||v_r|\sin(\theta_s - \theta_r) \\ \frac{\partial P_{ad_s}}{\partial D_s} = \frac{\left\{ -2n^2(1 - D_s)x_c[(D_{ij}k_1 - C_{ij}k_2) - 2C_{ij}E_{ij}x_{\text{series}}] \right\}}{\text{Den}} \\ \times |v_s||v_r|\cos(\theta_r - \theta_s) \\ + \frac{\left\{ [(D_{ij}k_1 - C_{ij}k_2)x_{\text{series}} - C_{ij}E_{ij}x_{\text{series}}^2] \right\}}{\text{Den}^2} \\ \times \left\{ 4n^2(1 - D_s)x_c(k_2 + E_{ij}x_{\text{series}}) \right\}|v_s||v_r|\cos(\theta_r - \theta_s) \\ + \frac{\left\{ -2n^2(1 - D_s)x_c[(C_{ij}k_1 + D_{ij}k_2) + 2D_{ij}E_{ij}x_{\text{series}}] \right\}}{\text{Den}} \\ \times |v_s||v_r|\sin(\theta_r - \theta_s) \\ + \frac{\left\{ [(C_{ij}k_1 + D_{ij}k_2)x_{\text{series}} + D_{ij}E_{ij}x_{\text{series}}^2] \right\}}{\text{Den}^2} \\ \times \left\{ 4n^2(1 - D_s)x_c(k_2 + E_{ij}x_{\text{series}}) \right\}|v_s||v_r|\sin(\theta_r - \theta_s) \\ + \frac{\left\{ -2n^2(1 - D_s)x_c[(C_{ij}k_4 - D_{ij}k_3) + 2(C_{ij}G_{ij} - D_{ij}F_{ij})x_{\text{series}}] \right\}}{\text{Den}}|v_r|^2 \\ + \frac{\left\{ [(C_{ij}k_4 - D_{ij}k_3)x_{\text{series}} + (C_{ij}G_{ij} - D_{ij}F_{ij})x_{\text{series}}^2] \right\}}{\text{Den}^2} \\ \times \left\{ 4n^2(1 - D_s)x_c(k_2 + E_{ij}x_{\text{series}}) \right\}|v_r|^2 \\ \frac{\partial Q_{ad_s}}{\partial D_s} = \frac{\left\{ -2n^2(1 - D_s)x_c[(D_{ij}k_1 - C_{ij}k_2) - 2C_{ij}E_{ij}x_{\text{series}}] \right\}}{\text{Den}} \\ \times |v_s||v_r|\sin(\theta_r - \theta_s) + \frac{\left\{ [(D_{ij}k_1 - C_{ij}k_2)x_{\text{series}} - C_{ij}E_{ij}x_{\text{series}}^2] \right\}}{\text{Den}^2} \\ \times \left\{ 4n^2(1 - D_s)x_c(k_2 + E_{ij}x_{\text{series}}) \right\}|v_s||v_r|\sin(\theta_r - \theta_s) \\ - \frac{\left\{ -2n^2(1 - D_s)x_c[(C_{ij}k_1 + D_{ij}k_2) + 2D_{ij}E_{ij}x_{\text{series}}] \right\}}{\text{Den}}$$

$$\begin{aligned}
& \times |v_s| |v_r| \cos(\theta_r - \theta_s) \\
& + \frac{\left\{ \left[ (C_{ij}k_1 + D_{ij}k_2)x_{\text{serie}} + D_{ij}E_{ij}x_{\text{serie}}^2 \right] \right.}{\text{Den}^2} \\
& \times \left[ 4n^2(1 - D_s)x_c(k_2 + E_{ij}x_{\text{serie}}) \right] \Big\} \\
& \times |v_s| |v_r| \cos(\theta_r - \theta_s) \\
& + \frac{\left\{ \begin{aligned} & -2n^2(1 - D_s)x_c \left[ (C_{ij}k_4 + D_{ij}k_3) \right] \\ & + 2(C_{ij}F_{ij} + D_{ij}G_{ij})x_{\text{serie}} \end{aligned} \right\}}{\text{Den}} |v_r|^2 \\
& + \frac{\left\{ \left[ (C_{ij}k_3 + D_{ij}k_4)x_{\text{serie}} + (C_{ij}F_{ij} + D_{ij}G_{ij})x_{\text{serie}}^2 \right] \right.}{\text{Den}^2} \\
& \times \left[ 4n^2(1 - D_s)x_c(k_2 + E_{ij}x_{\text{serie}}) \right] \Big\} |v_r|^2
\end{aligned}$$

Element  $j_{\text{III}}$

$$\begin{aligned}
\frac{\partial P_{\text{controlled}}}{\partial D_s} &= - \frac{2k_1 \left\{ 4x_c n^2 (1 - D_s) [k_2 + x_{\text{serie}} E_{ij}] \right\}}{\text{Den}^2} |v_s|^2 \\
&+ \frac{2F_{ij}x_c n^2 (1 - D_s)}{\text{Den}} |v_s| |v_r| \cos(\theta_s - \theta_r) \\
&- \frac{[k_3 + F_{ij}x_{\text{serie}}] \left\{ 4x_c n^2 (1 - D_s) [k_2 + x_{\text{serie}} E_{ij}] \right\}}{\text{Den}^2} \\
&\times |v_s| |v_r| \cos(\theta_s - \theta_r) \\
&+ \frac{2G_{ij}x_c n^2 (1 - D_s)}{\text{Den}} |v_s| |v_r| \sin(\theta_s - \theta_r) \\
&- \frac{[k_4 + G_{ij}x_{\text{serie}}] \left\{ 4x_c n^2 (1 - D_s) [k_2 + x_{\text{serie}} E_{ij}] \right\}}{\text{Den}^2} \\
&\times |v_s| |v_r| \sin(\theta_s - \theta_r)
\end{aligned}$$